INTERNATIONAL JOURNAL FOR NUMERICAL METHODS IN FLUIDS, VOL. 2, 367–386 (1982)

SURFACE TENSION DRIVEN FLOWS IN MICRO-GRAVITY CONDITIONS

M. STRANI* AND R. PIVA†
University of Rome, Italy

SUMMARY

The importance of convective flows generated by surface tension gradients, in comparison with the ones generated by other driving forces, has been investigated in connection with space technological applications involving fluid processes. A theoretical model of the boundary conditions at the interface, considered free and diffusive, has been derived in general tensor form to allow for the use of non-orthogonal curvilinear co-ordinates. For the study of flow fields contained in enclosures, these co-ordinates are more suitable to fit all the boundaries, in particular near the contact angle between the interface and the solid walls, thus giving more accurate numerical solutions.

A computational procedure to solve the complete set of bulk and surface equations is proposed and applied to a simplified two dimensional flow in a rectangular enclosure with a temperature gradient between the lateral walls. The numerical results show the importance of considering the interface to be deformable and diffusive for an accurate evaluation of the convective flow in the fluid bulk.

KEY WORDS Free Surface Thermocapillary Convective Flows Curvilinear Co-ordinates Interface Equations

1. INTRODUCTION

The interface between two immiscible fluids generally influences the motion within the adjacent fluids through its geometrical shape and the surface tension gradients which may be generated along the surface by temperature or concentration gradients. Surface tension gradients act as a shear stress at the surface itself, inducing significant convective flows besides the ones directly established by temperature and concentration gradients.

These flows become important in comparison with buoyancy convective flows for small values of the modified Bond number, defined as the ratio of gravitational to surface tension forces. Therefore they are significant or may even become predominant for relatively small characteristic dimensions of the flow field, e.g. liquid films, or for reduced gravity conditions. In the latter context a large interest has been recently dedicated to flow processes in space for technological applications regarding, for instance, crystal growth and new composite materials.

The effect of surface tension and its coupling with other driving forces may give rise to very complex flow phenomena which, in order to be controlled in technological applications, must be first investigated from a theoretical point of view with a sufficient level of completeness and accuracy. Considering that the surface tension driven motion is generated at the interface and, from there, it propagates into the fluid bulk, the application of proper boundary conditions at the interface plays a central role in the mathematical formulation of the problem.

* Istituto di Macchine e Tecnologie
† Istituto di Meccanica Applicata alle Macchine

0271–2091/82/040367–20$02.00

Received 6 July 1981
Revised 17 November 1981

Simplified interface balance equations have been used by several authors[1–3] as boundary conditions for analytical or numerical solutions of the bulk equations. The assumption of a fixed rectilinear configuration[4] or the discrete approximation in Cartesian co-ordinates of the interface,[5] viewed from the modern framework of sophisticated computational procedures, may not be adequate for an accurate simulation of the physical phenomena.

To overcome the difficulties connected with the curvilinear shape of the free boundary, two different approaches may be followed: finite element techniques, typically adopted for free boundary flows such as the die swell problem,[6–9] or a finite difference method based on a system of generalized co-ordinates with the free boundary coincident with a portion of a co-ordinate surface.

The computational procedure presented in this paper is based on the latter approach, whose relative advantages have been discussed elsewhere.[10,11]

A particular choice of generalized co-ordinates, based on the assumption of the stream function as one of the co-ordinates, has been proposed by Duda and Vrentas for the study of laminar liquid jets.[12] For complex flow fields with multiple recirculating regions, which may appear in surface tension driven flows in enclosures, a more general choice of boundary fitted co-ordinates must be assumed.

A general formulation of the dynamical boundary conditions on the interface between two immiscible fluids was first derived, in tensorial form, by Scriven.[13] The complete formulation of thermal and dynamical boundary conditions, with particular attention to non-equilibrium thermodynamic aspects, has been recently presented, in vectorial form and with reference to an orthogonal curvilinear co-ordinate system, by Bedeaux *et al.*,[14] and Napolitano.[15]

For the study of flow fields contained in enclosures, as we often find in applications, non-orthogonal curvilinear co-ordinates may better fit all the boundaries, in particular near the contact angle between the fluid interface and the solid wall.

The purpose of the present paper is, first, to derive the complete interface balance equations, in general tensorial form, which are valid for any non-orthogonal system of curvilinear co-ordinates, and second, to suggest a computational method for the solution of the complete set of bulk, interface and constitutive equations.

In particular, in Section 2, the co-ordinate systems, utilized in the mathematical formulation, are defined and the bulk conservation equations, written in tensorial form for generalized co-ordinates, are also recalled. The discontinuous model for the interface is discussed in Section 3, together with the derivation of the interface balance equations for mass, momentum and energy.

In Section 4, starting from the interface entropy balance equation, the linear constitutive laws for the surface quantities appearing in the mass, momentum and energy balance equations, are derived in the frame of irreversible thermodynamic processes.

A two dimensional sample flow with simplifying physical hypotheses is considered in Section 5 as a test case for the mathematical and computational model.

The main features of the computational model are briefly discussed in Section 6, while the numerical results for the sample flow are presented in Section 7.

2. CO-ORDINATE SYSTEMS AND BULK CONSERVATION EQUATIONS

The steady state motion of two immiscible fluids (+) and (−), separated by a surface S_2 of arbitrary shape, is considered in a three dimensional space S_3.

The surface B, the boundary of the domain containing both fluids, may be open when one or both fluids extend to infinity. Let $\langle x^k \rangle$ be a system of orthogonal Cartesian co-ordinates

defined in S_3. As usually assumed, latin indices range from 1 to 3, while greek indices range from 1 to 2.

Assuming the surface S_2 to be sufficiently smooth, we may consider in S_3 a system of generalized co-ordinates $\langle \xi^k \rangle$, in which the surface S_2 is a co-ordinate surface, e.g. it may be expressed as

$$\xi^3 = K \tag{1}$$

The symbols $(\ )^+$ and $(\ )^-$ indicate respectively the fluids in the space regions on the two sides of S_2; that is, for $\xi^3 > K$ and $\xi^3 < K$.

The co-ordinates ξ^k are related to the Cartesian co-ordinates x^k by the equations

$$x^k = x^k(\xi^1, \xi^2, \xi^3) \tag{2}$$

$$\xi^k = \xi^k(x^1, x^2, x^3) \tag{3}$$

where x^k and ξ^k are single valued and continuous differentiable functions.

The metric tensor components g^{ik} (or g_{ik}) define the metric in the physical space S_3.

In the two dimensional subspace S_2, given by equation (1), $\langle \xi^\alpha \rangle$ is a generalized co-ordinate system whose metric is defined by the contravariant components $\gamma^{\alpha\beta}$ (or covariant components $\gamma_{\alpha\beta}$) of the metric tensor.[16]

For a generalized co-ordinate system the bulk conservation equations for fluids (+) and (−), in the hypothesis of steady state conditions, may be written, in tensorial form[17]

$$(\phi^k)^{\pm}_{|k} = 0 \tag{4}$$

$$(\phi^{ik})^{\pm}_{|k} = 0 \tag{5}$$

with fluxes ϕ^k, ϕ^{ik} of scalar and vectorial quantities respectively given by

$$\phi^k = \rho u^k \qquad \text{for mass conservation}$$

$$\phi^k = \rho u^k \left(U + \frac{u^k u_k}{2} \right) + q^k - u_i \sigma^{ik} \qquad \text{for total energy conservation}$$

$$\phi^{ik} = \rho u^i u^k - \sigma^{ik} \qquad \text{for momentum conservation}$$

where the thermal flux q^k and the stress tensor σ^{ik} are given, for Newtonian bulk fluids, by the constitutive relations

$$q^k = -\lambda g^{hk} T_{,h}$$

$$\sigma^{ik} = (-p + (\mu_\nu - \tfrac{2}{3}\mu) u^m_{|m}) g^{ik} + \mu (u_{n|m} + u_{m|n}) g^{in} g^{km}$$

For each bulk fluid the thermodynamic variables U, p, T, and ρ are connected by two equations of state, while μ, μ_ν and λ have been assumed constant.

3. BALANCE EQUATIONS AT THE INTERFACE

From a purely macroscopic point of view the interface between two immiscible fluids is a particular case of a discontinuity surface S_2, where the tensor distributions ϕ^k, ϕ^{ik} in (4), (5) may become singular.

Under this hypothesis and by assuming the conservation equations to be valid everywhere in S_3, following the procedure indicated by Bedeaux *et al.*,[14] the set of surface balance equations, in tensorial form and with reference to the generalized system of co-ordinates

mentioned in Section 2, has been previously obtained by the authors[18] in the form:

$$\left[\frac{\phi^3}{\sqrt{g^{33}}}\right]^+_- + \tilde{\phi}^\alpha_{\|\alpha} = 0 \tag{6}$$

$$\left[\frac{\phi^{33}}{g^{33}}\right]^+_- + \tilde{\phi}^{\beta\alpha} b_{\beta\alpha} = 0 \tag{7}$$

$$\left[\frac{\phi^3_\gamma}{\sqrt{g^{33}}}\right]^+_- + \tilde{\phi}^\alpha_{\gamma\|\alpha} = 0 \tag{8}$$

where $\tilde{\phi}^\alpha$ and $\tilde{\phi}^{\alpha\beta}$ are the surface densities of the field tensors, and

$$\left[\ \right]^+_- = \left[\ \right]^+ - \left[\ \right]^-$$

The tangential surface balance equations (6) and (8) are the analogues of (4), (5) in the two-dimensional subspace S_2, and account for the existence of local sources whose intensity is equal to the net flux across the surface of the bulk field tensors.

Equation (7) is the surface balance in a direction orthogonal to the surface itself, and gives a condition on the curvature tensor of the surface, whose shape is *a priori* unknown.

The surface balance equations, in their general form (6)–(8) are now specified for the case of an interface between two immiscible fluids, with the following hypotheses:

(a) the interface S_2 is an impermeable surface, that is a stream surface at steady state;

(b) local thermodynamic equilibrium prevails for the surface phase, implying the definition of surface velocity v^α and surface temperature θ;

(c) surface density of mass, $\tilde{\rho}$, equals zero;

(d) surface density of energy, $\tilde{u} = \tilde{\rho}\tilde{U}$, and entropy $\tilde{s} = \tilde{\rho}\tilde{S}$, are different from zero.

For the mass conservation equation we therefore have $\phi^k = \rho u^k$, $\tilde{\phi}^\alpha = \tilde{\rho} v^\alpha$, and equation (6) becomes

$$\left[\frac{\rho u^3}{\sqrt{g^{33}}}\right]^+_- + (\tilde{\rho} v^\alpha)_{\|\alpha} = 0 \tag{9}$$

which, on account of hypotheses (c) and (a) is trivially satisfied with

$$(u^3)^+ = (u^3)^- = 0 \tag{10}$$

For the momentum conservation equation we have $\phi^{ik} = \rho u^i u^k - \sigma^{ik}$ and, under hypothesis (c), $\tilde{\phi}^{\alpha\beta} = -\tilde{\sigma}^{\alpha\beta}$, where $\tilde{\sigma}^{\alpha\beta}$ is the diffusive surface flux of momentum.

Taking into account for (10), equations (7), (8) become,

$$\left[\frac{\sigma^{33}}{g^{33}}\right]^+_- + \tilde{\sigma}^{\beta\alpha} b_{\beta\alpha} = 0 \tag{11}$$

$$\left[\frac{\sigma^3_\gamma}{\sqrt{g^{33}}}\right]^+_- + \tilde{\sigma}^\alpha_{\gamma\|\alpha} = 0 \tag{12}$$

For the energy conservation equation we have $\tilde{\phi}^\beta = \tilde{u} v^\beta + \tilde{q}^\beta - v_\alpha \tilde{\sigma}^{\alpha\beta}$, where, on account of hypothesis (c), the surface density of kinetic energy is zero and the surface diffusive energy flux has been divided into a mechanical and a thermal part.

Considering (10), equation (6) gives,

$$\frac{1}{\sqrt{g^{33}}}[q^3 - u_i \sigma^{i3}]^+_- + (\tilde{u} v^\alpha + \tilde{q}^\alpha - v_\beta \tilde{\sigma}^{\beta\alpha})_{\|\alpha} = 0 \tag{13}$$

The surface balance of the mechanical energy is obtained multiplying (12) by v_δ,

$$\tilde{\sigma}^{\delta\alpha}_{\|\alpha} v_\delta = \left[\frac{-\sigma^{3i} v_i}{\sqrt{g^{33}}}\right]^+_-$$

As a consequence, equation (13) may be written in the form

$$\frac{1}{\sqrt{g^{33}}}[q^3 - \sigma^{i3}(u_i - v_i)]^+_- + (\tilde{u}v^\alpha + \tilde{q}^\alpha)_{\|\alpha} - \tilde{\sigma}^{\delta\alpha} v_{\delta\|\alpha} = 0 \tag{14}$$

which expresses the surface balance of the thermal energy.

4. CONSTITUTIVE EQUATIONS AT THE INTERFACE

Surface diffusive fluxes $\tilde{q}^\alpha$ and $\tilde{\sigma}^{\alpha\beta}$ may be specified, in the frame of linear irreversible thermodynamics,[19] starting from the surface entropy production equation which, consistent with the above mentioned model of the interface, may be written as

$$-\frac{\sigma}{\theta} v^\alpha_{\|\alpha} - \frac{\tilde{q}^\alpha}{\theta^2}\theta_{,\alpha} + \frac{\tilde{\sigma}^{\delta\alpha}}{\theta} v_{\delta\|\alpha} + \frac{1}{\sqrt{g^{33}}} q^3 \left[\frac{1}{T} - \frac{1}{\theta}\right]^+_- + \frac{\sigma^{i3}}{\theta}[u^i - v^i]^+_- \geqslant 0 \tag{15}$$

After some manipulations, the entropy production term may be written as the sum of tensorial products between thermodynamic forces and fluxes.[18] The hypothesis of a Newtonian surface fluid phase thus leads, by neglecting the cross-effects, to the following set of constitutive equations:

$$\tilde{\sigma}^\alpha_\beta = (\sigma + \tfrac{1}{2}\tilde{\Pi}^\delta_\delta)\delta^\alpha_\beta + \tilde{\tilde{\Pi}}^\alpha_\beta \tag{16}$$

$$\tilde{q}^\alpha = -\lambda_s \gamma^{\alpha\beta}\theta_{,\beta} \tag{17}$$

$$\tfrac{1}{2}\Pi^\delta_\delta = \mu_{sv} v^\delta_{\|\delta} \tag{18}$$

$$\tilde{\tilde{\Pi}}^\alpha_\beta = \mu_s[(v_{\delta\|\beta} + v_{\beta\|\delta})\gamma^{\delta\alpha} - \delta^\alpha_\beta v^\gamma_{\|\gamma}] \tag{19}$$

$$\frac{(\sigma^3_\alpha)^+ + (\sigma^3_\alpha)^-}{2\sqrt{g^{33}}} = \beta[(u_\alpha)^+ - (u_\alpha)^-] \tag{20}$$

$$\frac{(\sigma^3_\alpha)^- - (\sigma^3_\alpha)^+}{\sqrt{g^{33}}} = \alpha_{33}\{v_\alpha - \tfrac{1}{2}[(u_\alpha)^+ + (u_\alpha)^-]\} \tag{21}$$

$$\frac{(q^3)^+ + (q^3)^-}{2\sqrt{g^{33}}} = -L_{22}\left(\frac{1}{T^-} - \frac{1}{T^+}\right) \tag{22}$$

$$\frac{(q^3)^+ - (q^3)^-}{\sqrt{g^{33}}} = -L_{33}\left[\frac{1}{\theta} - \frac{1}{2}\left(\frac{1}{T^+} + \frac{1}{T^-}\right)\right], \tag{23}$$

which connect thermodynamic forces to the corresponding thermodynamic fluxes.

Equations (16)–(19) are the constitutive relations for the surface stress tensor $\tilde{\sigma}^{\alpha\beta}$ and the surface heat flux $\tilde{q}^\alpha$, while (20)–(23) are the constitutive relations for the boundary values of σ^3_α and q^3 at the interface.

The balance equations (10)–(12) and (14) together with the constitutive equations (16)–(23), give a complete set of boundary conditions, at the free surface, for the bulk conservation equations (4), (5).

The present mathematical model of the interface accounts for a large set of physical phenomena, in particular the surface diffusive processes and the discontinuity between bulk

and surface velocities and temperatures, which, under certain circumstances, may give rise to significant effects on the flow field configuration.

This seems to be the case for surface tension driven flows, which require particular attention to the conditions at the free surface, where the driving forces are located.

5. A TWO-DIMENSIONAL SAMPLE FLOW

Let us assume, as a test case for a numerical application, a two-dimensional incompressible flow at zero gravity in the plane $x^1 = \text{constant}$, previously considered by the authors.[20]

A sketch of the physical and geometrical conditions of the flow field is shown in Figure 1.

The two fluids (+) and (−) separated by an interface, are contained in a rectangular enclosure open on the side of fluid (+). A temperature difference is imposed between the two lateral walls of the enclosure. At zero gravity no buoyancy forces appear, but the temperature difference induces a surface tension gradient along the interface, which drives a recirculating flow in the adjacent fluid bulks.

We assume that one of the two adjacent fluids, in particular fluid (+), has negligible effects on the interface, as would be the case for a perfect fluid at rest. This hypothesis allows us to consider only the bulk phase (−) and the surface phase, without any coupling with the flow field of fluid (+). It yields a simpler integration procedure from a numerical point of view, while maintaining most of the general features of the model. From a physical point of view this assumption may be reasonable if the viscous stress and the heat flux of fluid (+) at the interface may be neglected in comparison with the ones of fluid (−), as is the case, for instance, with an interface between air (+) and oil (−). In this hypothesis the pressure of fluid (+) may be considered constant and assumed as a reference pressure for the calculations.

Under these hypotheses the equations (20) and (21) combine to give the simpler relation

$$\frac{\sigma_2^3}{\sqrt{g^{33}}} = \frac{\alpha}{\gamma^{22}}(v_2 - u_2) \tag{24}$$

where $\frac{1}{\alpha} = \frac{1}{4\beta} + \frac{1}{\alpha_{33}}$, and the bulk quantities, from here on, refer to the fluid (−).

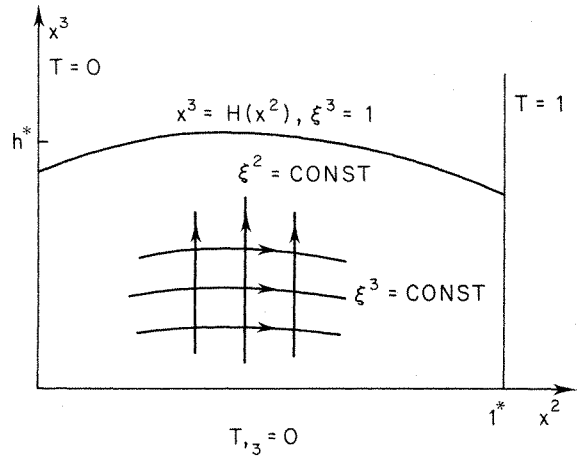

Figure 1. Sketch of the physical and geometrical conditions for the two-dimensional sample case

Analogously the combination of equations (22) and (23) gives

$$\frac{q^3}{\sqrt{g^{33}}} = L\left(\frac{1}{\theta} - \frac{1}{T}\right) \tag{25}$$

where

$$\frac{1}{L} = \frac{1}{L_{33}} + \frac{1}{4L_{22}}$$

In the present problem no velocity is imposed at the boundary. The Reynolds number of the flow, and consequently the reference velocity, must be chosen in an appropriate way to normalize the velocity field. As suggested by Ostrach,[2] if the surface tension Reynolds number defined as

$$R_\sigma = \sigma_{,T}\,|_{T_c}\,\Delta T l \rho / \mu^2$$

is sufficiently small, we obtain from the balance between viscous tangential stress and surface tension gradient at the interface, and for both terms to be of the same order of magnitude,

$$u_r = \sigma_{,T}\,|_{T_c}\,\Delta T / \mu$$

and, as a consequence the Reynolds number Re may be written as

$$Re = R_\sigma$$

Moreover, for the considered cases of low recirculating velocities, the Eckert number assumes a very small value and therefore all the terms proportional to it may be neglected.

With the above assumptions the complete set of field equations may thus be written in non-dimensional form (latin indices range from 1 to 2 for the 2-D flow),

$$\underline{u}^k_{|k} = 0 \tag{26}$$

$$\underline{u}^k \underline{u}^h_{|k} - \underline{\sigma}^{hk}_{|k} = 0 \tag{27}$$

$$\underline{u}^k \underline{T}_{,k} - \frac{1}{Ma}(g^{hk}\underline{T}_{,k})_{|h} = 0 \tag{28}$$

where $Ma = R_\sigma Pr$ is the Marangoni number and

$$\underline{\sigma}^{hk} = -\underline{p} g^{hk} + \frac{1}{R_\sigma}(\underline{u}_{n|m} + \underline{u}_{m|n}) g^{hn} g^{km} \tag{29}$$

while the boundary conditions at the free surface become

$$\underline{u}^3 = 0 \tag{30}$$

$$\frac{\underline{\sigma}^{33}}{g^{33}} - \frac{1}{R_\sigma}\tilde{\underline{\sigma}}^{22} b_{22} = 0 \tag{31}$$

$$\frac{\underline{\sigma}^3_2}{\sqrt{g^{33}}} + \frac{1}{R_\sigma}\tilde{\underline{\sigma}}^2_{2\|2} = 0 \tag{32}$$

$$\frac{\underline{q}^3}{\sqrt{g^{33}}} - (\tilde{\underline{q}}^2 + Ma\tilde{\underline{u}}\underline{v}^2)_{\|2} = 0 \tag{33}$$

with the constitutive relations

$$\tilde{\underline{\sigma}}_2^2 = \underline{\sigma} + \underline{\mu}_s(\underline{v}_{\|2}^2 + \underline{v}_{2\|2}\gamma^{22}) \tag{34}$$

$$\tilde{\underline{q}}_2 = -\underline{\lambda}_s \underline{\theta}_{,2} \tag{35}$$

$$\frac{\underline{\sigma}_2^3}{\sqrt{g^{33}}} = \underline{\alpha}(\underline{v}_2 - \underline{u}_2) \tag{36}$$

$$\frac{\underline{q}^3}{\sqrt{g^{33}}} = \underline{L}\left(\frac{1}{\underline{\theta} + \underline{T}_c} - \frac{1}{\underline{T} + \underline{T}_c}\right) \tag{37}$$

A linear relation between surface tension and temperature is assumed

$$\underline{\sigma} = \frac{1}{Cr} - \underline{T} \tag{38}$$

where the Crispation number Cr is given by

$$Cr = \sigma_{,T}\,|_{T_c}\,\Delta T/\sigma\,|_{T_c}$$

The surface balance equations (30), (32), (33) are boundary conditions at $\xi^3 = K$ for the bulk conservation equations: from their solution the boundary values of the two bulk velocity components $\underline{u}^2$, $\underline{u}^3$ and of the bulk temperature $\underline{T}$, are obtained.

We may observe that, besides the bulk quantities, the surface velocity, $\underline{v}^2$, and the surface temperature, $\underline{\theta}$, appear in these equations as further unknowns to be determined. Accounting also for the constitutive relations (36), (37) on the boundary values of $\underline{\sigma}_2^3$ and q^3 at the free surface, we may easily verify that the number of equations is sufficient to determine all the unknown boundary values at the interface. In particular for the velocity field, with $\underline{u}^3 = 0$ from equation (30), the two remaining components $\underline{u}^2$ and $\underline{v}^2$ are determined by the two equations (32) (after substitution of (34)) and (36). For the temperature, the surface and bulk boundary values $\underline{\theta}$ and $\underline{T}$, are determined from the two equations (33) (after substitution of (35)) and (37).

The remaining surface balance equation (31) determines the unknown component $\underline{b}_{22}$ of the curvature tensor $\underline{b}_{\beta\alpha}$ of the surface S_2, and, with the appropriate boundary conditions about the contact angle at the solid walls, its unknown geometrical shape

$$\underline{x}_s^k = \underline{x}_s^k(\xi^1, \xi^2)$$

in the Cartesian co-ordinate system $\langle \underline{x}^k \rangle$. The metric coefficients and Christoffel symbols that appear in the differential equations and boundary conditions may be expressed as function of $\underline{x}_s^K$ and its derivatives.

It can easily be recognized that the simplified set of boundary conditions at the interface, which follow from the hypotheses

$$\tilde{\underline{\sigma}}_2^2 = \underline{\sigma} \qquad \tilde{\underline{q}}^2 = 0 \qquad \underline{T}\,|_{\xi^3 = K} = \underline{\theta} \qquad \underline{u}^2\,|_{\xi^3 = K} = \underline{v}^2$$

most frequently assumed in the literature on this subject, are immediately obtained from (30)–(37) for $\underline{\lambda}_s \to 0$, $\underline{\mu}_s \to 0$, $\underline{\alpha} \to \infty$, $\underline{L} \to \infty$.

The mathematical model described in this section, although simplified with respect to the general one, still leads to a very complicated set of equations which requires the adoption of a numerical integration procedure. The main features of the finite difference computational method are discussed in the following sections together with the most significant numerical results obtained for the considered sample case.

6. COMPUTATIONAL PROCEDURE

Co-ordinate transformation

The map from the field domain in the physical space $\langle x^k \rangle$ to a domain bounded by portions of co-ordinate surfaces in the transformed space $\langle x^k \rangle$, is performed through the analytical functions

$$\underline{x}^2 = \frac{x^2}{l} = f(\underline{\xi}^2) \tag{39}$$

$$\underline{x}^3 = \frac{x^3}{h} = \underline{H}(f(\underline{\xi}^2))t(\underline{\xi}^3) \tag{40}$$

where h and l are the average height and the length indicated in Figure 1. $\underline{H}(\underline{x}^2)$ is a continuous differentiable single valued function representing the interface geometrical configuration, while $f(\underline{\xi}^2)$, $t(\underline{\xi}^3)$ are two stretching functions which allow for non-uniform mesh size in the integration domain. The following stretching functions have been adopted for the present numerical results

(a) $f(\underline{\xi}^2) = \underline{\xi}^2 \qquad t(\underline{\xi}^3) = \underline{\xi}^3$

that give a uniform mesh size, or

(b) $$f(\underline{\xi}^2) = \frac{\tanh\left[C_x(\underline{\xi}^2 - 0{\cdot}5)\right] + \tanh\left(0{\cdot}5\, C_x\right)}{2\tanh\left(0{\cdot}5\, C_x\right)} \qquad t(\underline{\xi}^3) = \frac{\tanh\left(C_y \underline{\xi}^3\right)}{2\tanh\left(C_y\right)}$$

that give smaller mesh sizes near the fixed and free boundaries. The values of the two constants C_x, C_y determine the stretching intensity in x and y directions, respectively.

The metric tensor components and the Christoffel symbols for both space and surface co-ordinate systems, are easily determined by successive derivations of the functions (39) and (40).[16]

A numerical generation of boundary fitted co-ordinates could be efficiently obtained with the method proposed by Thames *et al.*[21] in the presence of more complex boundary shapes, as may occur, for instance, if $\underline{H}(\underline{x}^2)$ is not a single valued function.

Discretization schemes

For the integration of the bulk conservation equations, (26)–(29), the contravariant velocity components $\underline{u}^k$, the pressure $\underline{p}$ and the temperature $\underline{T}$, are assumed as field variables. In the discretization scheme they are localized on independent meshes shifted with respect to a reference cell, to reproduce the proper extension of the MAC method[22] to curvilinear co-ordinates, as indicated by Piva *et al.*[10] in a finite element context. In fact the contravariant velocity components, directly connected to the mass fluxes across the cell sides, are located at cell midsides, while the pressure and temperature are located at the centre of the cell.

The metric coefficients which are associated with all variables in the equations need to be calculated both at the centre of the cell and at the cell midsides, thus in a grid twice as fine as the one adopted for the physical variables. Analogously, the surface variables $\underline{\sigma}$, $\underline{\theta}$ and $\underline{v}^2$ are defined respectively at the step centre and at the nodes of the surface grid.

Integration procedure

The steady state momentum and energy conservation equations for the fluid bulk are integrated by a standard time-dependent-like iterative procedure, which satisfies, at each

time step, the mass conservation equation up to a certain level with successive iterations over a simplified set of equations.[23]

The boundary values of the field variables are obtained, at each iteration step, by a finite difference approximation of equations (30)–(37) for the free boundary, and of the following boundary conditions for the solid walls.

$$\text{(a)}\quad \begin{aligned} &\underline{u}^2 = \underline{v}^2 = 0, \\ &\underline{T} = \theta = \underline{\xi}^2, \\ &\underline{T}_{,3} = 0, \\ &\underline{u}^2 = \underline{u}^3 = 0, \end{aligned} \qquad \text{(b)}\quad \begin{aligned} &\underline{\xi}^2 = 0, 1 \\ &\underline{\xi}^2 = 0, 1 \\ &\underline{\xi}^3 = 0 \\ &\underline{\xi}^3 = 0 \end{aligned}$$

For the velocity interface conditions the finite difference approximation of (32), (34), (36), gives two coupled tridiagonal sets of linear equations in the unknowns $\underline{u}^2$ and $\underline{v}^2$, that can be written as

$$-A(i)\underline{u}^2(i+1) + B(i)\underline{u}^2(i) - C(i)\underline{u}^2(i-1) + Q(i)\underline{v}^2(i) = D(i) \tag{41}$$

$$-a(i)\underline{v}^2(i+1) + b(i)\underline{v}^2(i) - c(i)\underline{v}^2(i-1) + q(i)\underline{u}^2(i) = d(i) \qquad (i = 2, IF-1) \tag{42}$$

with the conditions at the solid walls ($i = 1$, $i = IF$)

$$\underline{u}^2(1) = \underline{v}^2(1) = 0 \tag{43}$$

$$\underline{u}^2(IF) = \underline{v}^2(IF) = 0 \tag{44}$$

The coupled system (41)–(44) has been solved with a procedure, described in the Appendix, that generalizes the well known tridiagonal algorithm.[24]

For the temperature interface conditions, a linearization of (37) has been used assuming as unknowns the values $\Delta\underline{T}$ and $\Delta\underline{\theta}$, respectively, of the bulk and surface temperature differences between two successive time iteration steps. By a proper assumption of the initial temperature distribution, $\Delta\underline{T}$ and $\Delta\underline{\theta}$ are always small enough to neglect higher order terms. The finite difference approximation of (33), (35), (37) is reduced to a tridiagonal coupled system of equations in $\Delta\underline{T}$ and $\Delta\underline{\theta}$ exactly analogous to (41)–(44) and solved with the same procedure.

At each iteration step the geometrical configuration $\underline{H}(\underline{x}^2)$ of the interface, consistent with the approximate flow field, can be determined by the integration of equation (31). The pressure in the bulk field is determined with respect to a value $\underline{p}_0$, which is an unknown parameter of the second order non-linear differential equation in $\underline{H}(\underline{x}^2)$. Accounting for the expressions of $\underline{\sigma}^{33}$, $\underline{\tilde{\sigma}}^{22}$ and $\underline{b}_{22}$, equation (31) can be written, in the absence of mesh stretching, as

$$\mathrm{y} = a\underline{H}_{,x} \tag{45}$$

$$\mathrm{y}_{,x} + \frac{\underline{p}_0 - B(x)}{A(x)}(1 + \mathrm{y}^2)^{3/2} = 0 \tag{46}$$

where $B(x)$, $A(x)$ are known functions at each time step, and the co-ordinate $\underline{x}^2$ is hereafter indicated as $x = \underline{x}^2$. The following wall boundary conditions are associated with equations (45) and (46).

$$\mathrm{y}(0) = a\underline{H}_{,x}(0) = \mathrm{y}_0 \tag{47}$$

$$\mathrm{y}(1) = a\underline{H}_{,x}(1) = \mathrm{y}_1, \tag{48}$$

as well as the condition of total fluid volume conservation,

$$\int_0^1 \underline{H}(x)\,dx = 1 \tag{49}$$

The system (47)–(49) is solved through a semi-analytical technique. In fact the solution of (46)–(48) is given by

$$\frac{y}{(1+y^2)^{1/2}} - \frac{y_0}{(1+y_0^2)^{1/2}} = -\underline{p}_0 \int_0^x \frac{dx}{A(x)} + \int_0^x \frac{B(x)}{A(x)}\,dx \tag{50}$$

where $\underline{p}_0$ is determined by

$$\frac{y_1}{(1+y_1^2)^{1/2}} - \frac{y_0}{(1+y_0^2)^{1/2}} = -\underline{p}_0 \int_0^1 \frac{dx}{A(x)} + \int_0^1 \frac{B(x)}{A(x)}\,dx \tag{51}$$

Equation (51) is a dynamical balance for the entire interface in the x^3 direction. The function $\underline{H}(x)$ follows immediately from (45) and (49).

Test case for the numerical procedure

The computational model has been tested first with reference to the asymptotic case of $a = \dfrac{h}{l} \to 0$ for which an analytical solution has been given by Levich.[25] In this solution, the velocity and the pressure gradient in the central region of the enclosure are expressed by

$$\underline{u}^2 = \frac{a}{4R_\sigma}\frac{d\underline{\sigma}}{dx}(-2y+3y^2) \tag{52}$$

$$\frac{d\underline{p}}{dx} = \frac{3}{2aR_\sigma}\frac{d\underline{\sigma}}{dx} \tag{53}$$

The analytical solution is compared in Table I with the one obtained from the computational model in which the following values of the parameters were assumed

$$R_\sigma = 2 \qquad Pr = 1 \qquad \underline{\lambda}_s = \underline{\mu}_s = 0 \qquad \underline{\alpha} = \underline{L} = 1 \qquad a = 0{\cdot}1 \qquad \frac{d\underline{\sigma}}{d\underline{x}} = -0{\cdot}1$$

The numerical results, reported in Table I, correspond to the centreline of the enclosure.

Table I

$\underline{y} = y/h$	$\underline{u}^2 \times 10^{-2}$ (52)	$\underline{u}^2 \times 10^{-2}$ (numerical solution)	$\dfrac{d\underline{p}}{dx}$ (53)	(numerical solution)
0	0	0		
0·1	0·425	0·435		
0·2	0·700	0·692		
0·3	0·825	0·812		
0·4	0·800	0·783		
0·5	0·625	0·609	−7·5	−7·4
0·6	0·300	0·287		
0·7	−0·175	−0·183		
0·8	−0·800	−0·804		
0·9	−1·575	−1·570		
1·0	−2·500	−2·510		

7. NUMERICAL RESULTS FOR THE SAMPLE FLOW

Several numerical results are presented and discussed in this section to assess the ability of the proposed numerical model to simulate, with a relatively small number of mesh points, the flow field even in the case of large deformation of the free surface.

The effects of the surface diffusive processes on the flow field configuration are also investigated to emphasize their relevance under certain physical conditions. A more systematic analysis of the ranges of variability for the non-dimensional parameters introduced in the mathematical model will be successively illustrated by the authors in a paper under preparation.

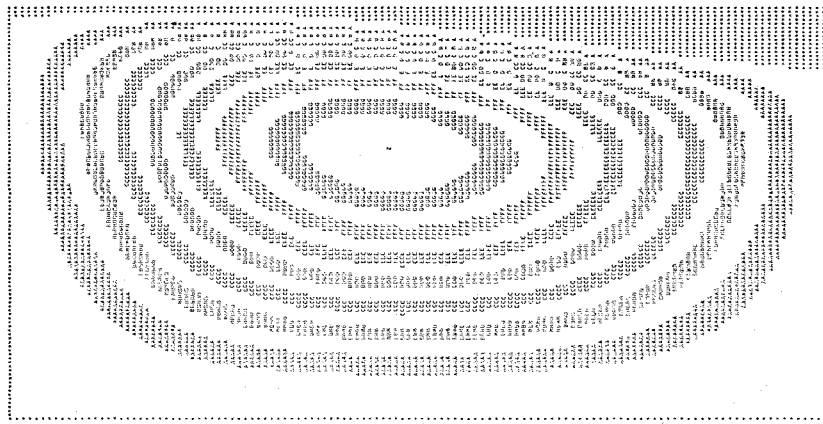

Figure 2. Streamline computer plot for $R_\sigma = 20$, $Pr = 1$, $a = 0{\cdot}5$, $Cr = 0{\cdot}5$ and free diffusive interface

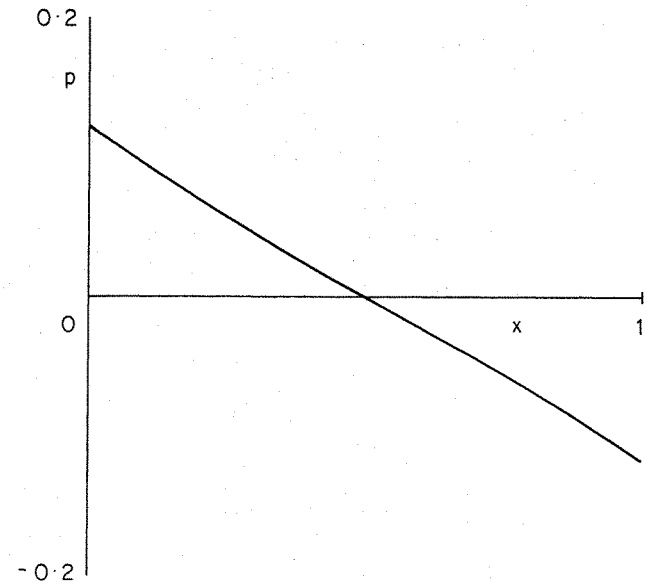

Figure 3. Bulk pressure distribution along the interface. $R_\sigma = 20$, $Pr = 1$, $a = 0{\cdot}5$, $Cr = 0{\cdot}5$ and free diffusive interface

The numerical values of the diffusive surface coefficients $\underline{\lambda}_s$, $\underline{\mu}_s$, $\underline{\alpha}$, $\underline{L}$, are not generally known. A unit reference value has been therefore assumed for the surface coefficients ($\underline{\lambda}_s = \underline{\mu}_s = \underline{\alpha} = \underline{L} = 1$) for the case of diffusive interface. As illustrated in Section 5 the non-diffusive interface is given by the values $\underline{\lambda}_s = \underline{\mu}_s = 0$ and $\underline{\alpha} = \underline{L} = 0{\cdot}8 \times 10^4$.

According to the reference velocity assumed in Section 5, the Reynolds number is always equal to the surface tension Reynolds number, while a unit value of the Prandtl number is assumed for all calculations.

The flow field for values of $R_\sigma = 20$, $a = 0{\cdot}5$, $Cr = 0{\cdot}5$ is first considered. An extreme value of the Crispation number, corresponding to very small surface tension and very large temperature gradients, has been assumed to enhance the effects of the surface deformation in comparison with the case of a flat undeformed surface, in order to test the capability of the proposed numerical method.

The computer plot of the streamline field, obtained with a (10×10) grid (Figure 2) shows the deformation of the interface boundary. The recirculating flow gives rise to approximately linear pressure distribution along the surface, with a maximum on the left side of the enclosure (Figure 3), which models the shape of the interface itself. Temperature and velocity vertical profiles at the enclosure centreline present the characteristic behaviour of recirculating flows. Velocity and temperature profiles at the section of maximum longitudinal velocity are shown quantitatively in Figures 4 and 5, where the numerical results for a flat non-diffusive interface and three values of $R_\sigma(2, 100, 600)$ are compared.

From the order of magnitude of the maximum velocity at the various R_σ it follows that, in the assumed range of relatively low values of R_σ, the reference velocity has been properly chosen.

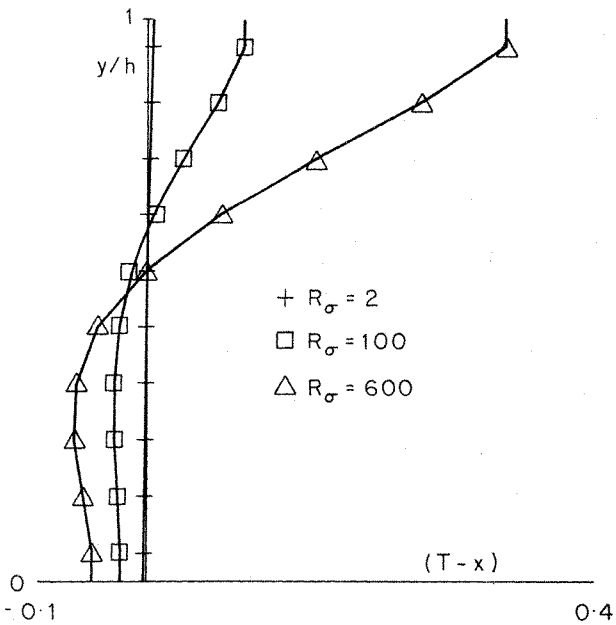

Figure 4. Temperature profiles for increasing Reynolds numbers: comparison between $R_\sigma = 2$, $R_\sigma = 100$, $R_\sigma = 600$

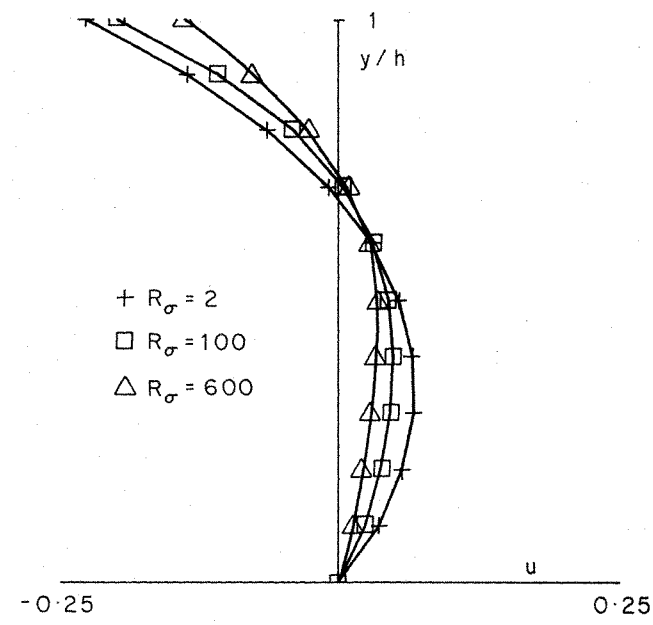

Figure 5. Velocity profiles for increasing Reynolds numbers: comparison between $R_\sigma = 2$, $R_\sigma = 100$, $R_\sigma = 600$

The surface temperature θ and surface velocity v^2 may differ significantly, in the case of a diffusive interface, from the corresponding bulk values at the free surface, as shown in Figure 6. In particular the surface velocity is always negative with absolute value larger than the bulk velocity, giving, for equation (36), a negative value of the stress component $\underline{\sigma}_2^3$ acting on the bulk fluid. On the contrary the surface temperature $\underline{\theta}$ is everywhere lower than the bulk temperature $\underline{T}$, and as a consequence a positive value of the heat flux component $\underline{q}^3$ results from equation (37).

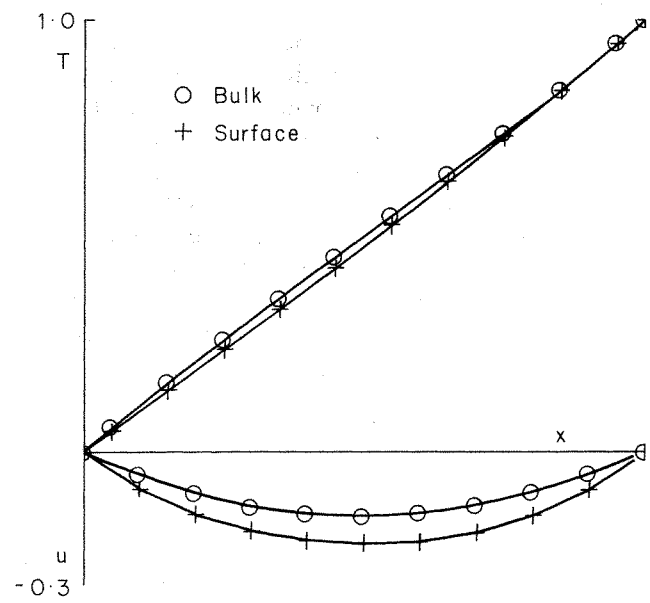

Figure 6. Distribution of bulk and surface temperature and of bulk and surface velocity along the interface for $R_\sigma = 20$, $Pr = 1$, $a = 0{\cdot}5$ and free diffusive interface

It is interesting to notice that the interface displacement and the surface diffusivity which are important characteristics of the present model, may have a strong influence on the bulk flow field. In fact, if we assume a flat undeformable and non-diffusive interface, as usually considered in other computational models, we obtain a flow field with a larger recirculating velocity as illustrated by the comparison of velocity and temperature profiles for the case of $R_\sigma = 20$, and $a = 0{\cdot}5$ (Figures 7, 8).

The comparison clearly indicates that the convective motions may be largely overestimated by the adoption of a too simplified physical and computational model. This result, which is confirmed by some recent expèriments on surface tension driven flows in a $NaNO_3$ melt,[26] could be of relevant importance for the technological applications where such convective motions are in general not desired.

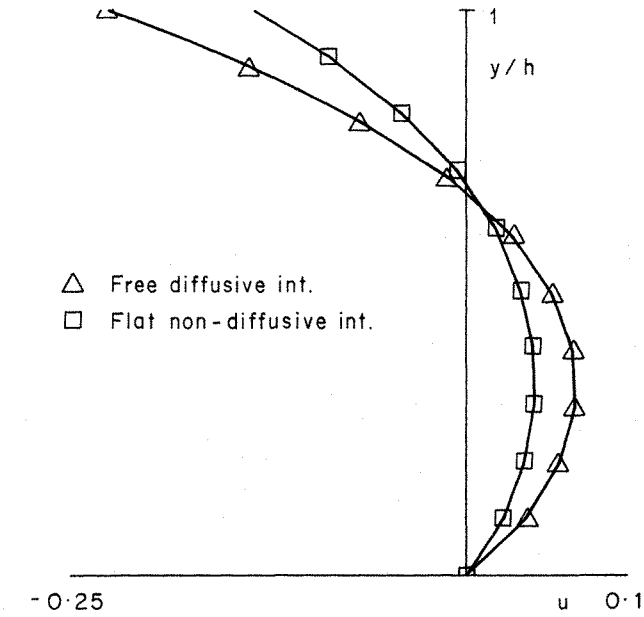

Figure 7. Comparison of velocity profiles at $\underset{\sim}{x} = 0{\cdot}5$ between the fields with free diffusive interface and flat non-diffusive interface for $R_\sigma = 20$, $Pr = 1$, $a = 0{\cdot}5$.

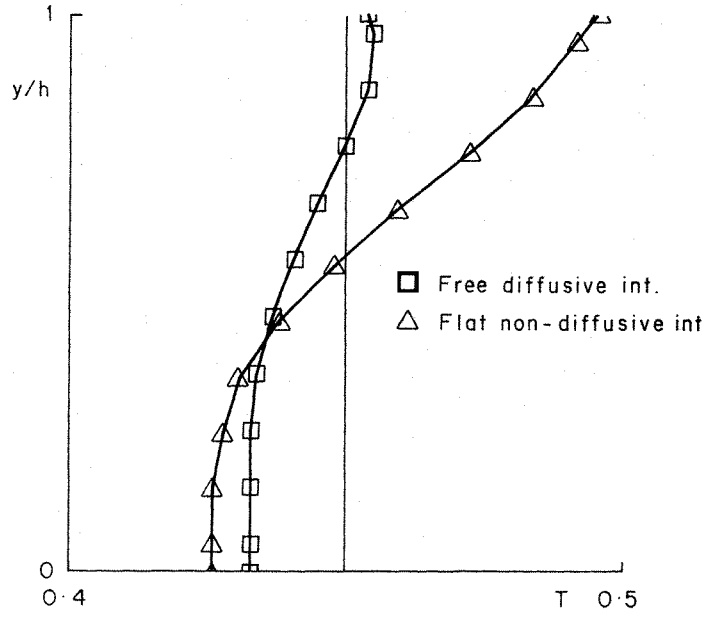

Figure 8. Comparison of temperature profiles at $\underset{\sim}{x} = 0{\cdot}45$ between the fields with free diffusive interface and flat non-diffusive interface for $R_\sigma = 20$, $Pr = 1$, $a = 0{\cdot}5$.

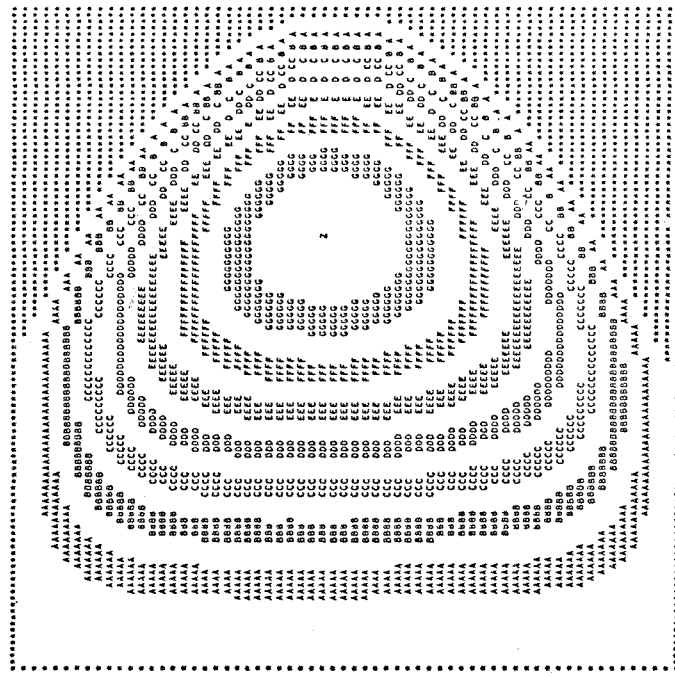

Figure 9. Streamlines computer plot, $R_\sigma = 20$, $Pr = 1$, $a = 0{\cdot}2$, $Cr = 0{\cdot}02$. The tangent of the contact angle is set equal to 0·25

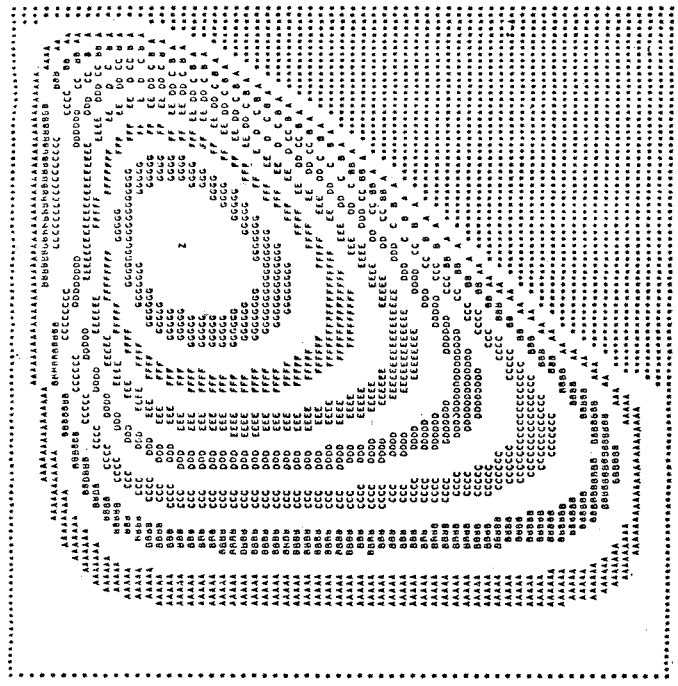

Figure 10. Streamlines computer plot, $R_\sigma = 15$, $Pr = 1$, $a = 0{\cdot}2$, $Cr = 0{\cdot}33$. The tangent of the contact angle is set to zero

The computational model appears to be particularly appropriate for flow fields with large deformations of the free surface. Figures 9 and 10 show the computer plots for the streamline field in two different cases (different scales are used in x and y directions). In the first (Figure 9) the large deformation of the surface is essentially due to the large values imposed for the contact angles. In the second (Figure 10), where a zero contact angle and a relatively large value of the Crispation number have been assumed, the large deformation is essentially caused by the dynamic pressure. Figure 11 shows the plot of surface velocities and temperatures for both cases.

It seems worth repeating that both flow fields were obtained using only a 10×10 mesh, analytically stretched only in the x direction.

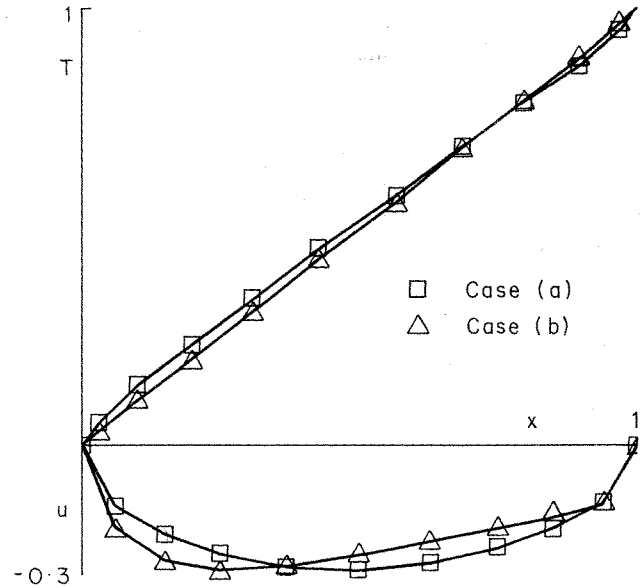

Figure 11. Surface velocity and temperature profiles along the interfaces in the cases of Figure 8, case (a), and Figure 9, case (b)

8. CONCLUDING REMARKS

The present invariant tensorial form of the field equations and boundary conditions allows the adoption of a boundary-conforming generalized system of co-ordinates, where free and solid boundaries are coincident with portions of the co-ordinate surfaces. The numerical integration of the free boundary problem is then performed through a standard finite difference scheme in the transformed space $\langle \xi^k \rangle$, with an accurate numerical approximation of the interface shape and of the associated boundary conditions in their most complete form. Efficient numerical solutions are obtained, with a comparatively low computer effort in comparison to other approaches.

The numerical results illustrated in the previous section, although limited to the particular physical case in which the effect of bulk fluid (+) may be neglected, show the capabilities of the proposed computational model. For this sample flow, in fact, an accurate description of

the flow field, that accounts for surface diffusive processes, has been obtained with a quite coarse mesh plus an appropriate stretching near the boundaries.

The discussion of the numerical results shows that the usual assumption of flat non-diffusive interface is, in general, not acceptable.

A deeper and systematic investigation would be required for evaluating the influence on thermocapillary flows of the values assumed for the coefficients appearing in the constitutive relations. The effect of the gravity force, although very small, is also a matter of further investigation, for the importance of the coupling effects of buoyancy and surface tension driven flows.

LIST OF SYMBOLS

$\langle x^k \rangle$	Cartesian co-ordinates system
$\langle \xi^k \rangle$	generalized co-ordinate system
$\langle \xi^\alpha \rangle$	generalized co-ordinate system on the interface
$(\ )_{,k}$	partial derivative with respect to ξ^k
$g^{ik}(\gamma^{\alpha\beta})$	metric tensor components in $\langle \xi^k \rangle (\langle \xi^\alpha \rangle)$
$(\ )_{\vert k}$	covariant derivative with respect to ξ^k in the metric of $\langle \xi^k \rangle$
$(\ )_{\Vert \alpha}$	covariant derivative with respect to ξ^α in the metric of $\langle \xi^\alpha \rangle$
$b_{\beta\alpha}$	interface curvature tensor components
ρ	density in the bulk
T	temperature in the bulk
θ	temperature on the interface
$u^k(u_k)$	contravariant (covariant) velocity components in the bulk
$v^\alpha(v_\alpha)$	contravariant (covariant) velocity components on the interface
σ^{ik}	contravariant components of the bulk stress tensor
$\tilde{\sigma}^{\alpha\beta}$	contravariant components of the surface stress tensor
p	pressure in the bulk
σ	surface tension
q^k	heat flux in the bulk
$\tilde{q}^\alpha$	heat flux on the interface
$\mu(\mu_s)$	bulk (surface) viscosity coefficient
$\lambda(\lambda_s)$	bulk (surface) coefficient of thermal conduction
$\underline{(\ )}$	non-dimensional variables
$Re = \rho u_r l/\mu$	Reynolds number
$R_\sigma = \sigma_{,T}\vert_{T_c} \Delta T l \rho/\mu^2$	surface tension Reynolds number
$Pr = \mu C_p/\lambda$	Prandtl number
$Cr = \sigma_{,T}\vert_{T_c} \Delta T/\sigma\vert_{T_c}$	Crispation number
$a = h/l$	aspect ratio
$Ma = R_\sigma Pr$	Marangoni number

APPENDIX

The coupled tridiagonal system in the unknowns $x(i)$, $y(i)$ $(i = 1, M)$

$$-A_i y(i+1) + B_i y(i) - C_i y(i-1) + Q_i x(i) = D_i \qquad (i = 2, M-1) \tag{54}$$

$$-a_i x(i+1) + b_i x(i) - c_i x(i-1) + q_i y(i) = d_i \tag{55}$$

with the boundary conditions

$$x(1) = x_1 \tag{56}$$

$$y(1) = y_1 \tag{57}$$

$$x(M) = x_M \tag{58}$$

$$y(M) = u_M \tag{59}$$

is a particular case of the block-tridiagonal system, for which the inversion procedure is well known.

However the solution algorithm assumes, for the system (54) and (55), a very simple form by setting

$$x(i) = e(i)x(i+1) + g(i)y(i+1) + f(i) \tag{60}$$

$$y(i) = E(i)y(i+1) + G(i)x(i+1) + F(i) \tag{61}$$

following the method[24] for tridiagonal systems of which (60) and (61) could be considered a generalization.

After substitution of (60), (61) in (54), (55), the following identities hold

$$e(i) = \frac{-a_i(B_i - C_iE(i-1))}{(Q_i - C_iG(i-1))(q_i - c_ig(i-1)) - (b_i - c_ie(i-1))(B_i - C_iE(i-1))} \tag{62}$$

$$g(i) = \frac{A_i(q_i - c_ig(i-1))}{(Q_i - C_iG(i-1))(q_i - c_ig(i-1)) - (b_i - c_ie(i-1))(B_i - C_iE(i-1))} \tag{63}$$

$$f(i) = \frac{(D_i + C_iF(i-1))(q_i - c_ig(i-1)) - (d_i + c_if(i-1))(B_i - C_iE(i-1))}{(Q_i - C_iG(i-1))(q_i - c_ig(i-1)) - (b_i - c_ie(i-1))(B_i - C_iE(i-1))} \tag{64}$$

$$E(i) = \frac{-A_i(b_i - c_ie(i-1))}{(Q_i - C_iG(i-1))(q_i - c_ig(i-1)) - (b_i - c_ie(i-1))(B_i - C_iE(i-1))} \tag{65}$$

$$G(i) = \frac{a_i(Q_i - C_iG(i-1))}{(Q_i - C_iG(i-1))(q_i - c_ig(i-1)) - (b_i - c_ie(i-1))(B_i - C_iE(i-1))} \tag{66}$$

$$F(i) = \frac{(d_i + c_if(i-1))(Q_i - C_iG(i-1)) - (D_i + C_iF(i-1))(b_i - c_ie(i-1))}{(Q_i - C_iG(i-1))(q_i - c_ig(i-1)) - (b_i - c_ie(i-1))(B_i - C_iE(i-1))} \tag{67}$$

After these substitutions, the same procedure of the above mentioned tridiagonal algorithm may be adopted for the solution.

REFERENCES

1. V. G. Levich and V. S. Krilov, 'Surface tension driven phenomena', *Ann. Rev. Fluid Mech.*, **1,** 293–316 (1969).
2. S. Ostrach, 'Motion induced by capillarity', *Proceedings of the International Conference on Physico-Chemical Hydrodynamics 1977*, Advance Publications, U.K., 1978.
3. L. E. Scriven, 'Drops and bubbles: their science and the system they model', *Prot. Int. Coll. On Drops and Bubbles*, **I,** 35–49, Calif. Inst. of Tech. and J.P.L., Aug. 1974.
4. C. E. Chang and W. R. Wilcox, 'Analysis of surface tension driven flow in floating zone melting', *Int. J. Heat Mass Transfer*, **19,** 355–366 (1976).
5. B. J. Daly, 'A technique for including surface tension effect in hydrodynamic calculations', *J. Compt. Physics*, **4,** (1), 97–117 (1969).
6. R. E., Nickell, R. I. Tanner and B. Caswell, 'The solution of viscous incompressible jet and free-surface flows using finite-element methods', *J. Fluid Mech.*, **65,** 189–206 (1974).
7. K. R. Reddy and R. I. Tanner, 'Finite element solution of viscous jet flows with surface tension', *Computers and Fluids*, **6,** 83–91 (1978).
8. P. W. Chang, T. W. Patten and B. A. Finlayson, 'Collocation and Galerkin finite element methods for viscoelastic fluid flow', Part I–II, *Computers and Fluids*, **7,** 267–293 (1979).

9. B. J. Omodei, 'Computer solutions of a plane Newtonian jet with surface tension', *Computers and Fluids*, **7,** 79–96 (1979).
10. R. Piva, A. Di Carlo and G. Guj, 'Finite element MAC scheme in general curvilinear coordinates', *Computers and Fluids*, **8,** 225–241 (1980).
11. A. Di Carlo, R. Piva and G. Guj, 'Computational schemes in general curvilinear coordinates for Navier-Stokes flows', *GAMM 1979, Notes in Numerical Fluid Mechanics*, **2,** 36–44, Vieveg Verlag Berlin.
12. J. L. Duda and J. S. Vrentas, 'Fluid mechanics of laminar liquid jets', *Chem. Engng. Sci.*, **22,** 855–869 (1967).
13. L. E., Scriven, 'Dynamics of a fluid interface', *Chem. Engng. Sci.*, **12,** 98–108 (1960).
14. D. Bedeaux, A. M. Albano and P. Mazur, 'Boundary conditions and non equilibrium thermodynamics', *Physica* **82A,** 438–462 (1976).
15. L. G. Napolitano, 'Thermodynamics and dynamics of pure interfaces', *Acta Astronautica*, **5,** (9), 655–670 (1978).
16. R. Aris, *Vectors, Tensors, and the Basic Equations of Fluid Mechanics*, Prentice-Hall, Englewood Cliffs, N.J., 1962.
17. J. C. Slattery, *Momentum, Energy, and Mass Transfer in Continua*, McGraw-Hill, Kogakusha, Tokyo, 1972.
18. M. Strani and R. Piva, 'A general formulation of boundary conditions at fluid interfaces', *AIDAA 5th National Congress*, Milan, 1979.
19. S. R. De Groot and P. Mazur, *Non Equilibrium Thermodynamics*, North-Holland, Amsterdam, 1962.
20. M. Strani and R. Piva, 'Computational models for convective motions induced at fluid interfaces', *Lecture Notes in Physics*, 141, p. 393, Springer Verlag, 1980.
21. F. C. Thames, J. F. Thompson, C. W. Mastin and R. L. Walker, 'Numerical solution for viscous and potential flow about two-dimensional bodies using body-fitted coordinate systems', *J. Comp. Physics*, **24,** 245–273 (1977).
22. F. H. Harlow and J. E. Welch, 'Numerical calculation of time dependent viscous incompressible flow of fluid with free surface', *The Physics of Fluids*, **8,** (12), 2182–2189 (1965).
23. C. W. Hirt and J. L. Cook, 'Calculating three-dimensional flows around structures and over rough terrain', *J. Comp. Physics*, **10,** 324–340 (1972).
24. R. D. Richtmeier and K. W. Morton, *Difference methods for Initial-value Problems*, Wiley New York 1967.
25. V. G. Levich, *Physicochemical Hydrodynamics*, Prentice Hall, 1962.
26. D. Schwabe and A. Scharmann, 'Marangoni convection in open boat and crucible', *Journal of Crystal Growth*, **52,** 435–449 (1981).